纤维与基体性能对炭纤维增强树脂基复合材料抗压强度的影响

李爱军[1,2]， 张军军[1]， 张方舟[2]， 李 龙[3]， 朱世鹏[3]， 杨云华[3]

（1. 上海大学 材料科学与工程学院，上海 200444；
2. 上海大学 材料研究所，上海 200072；
3. 航天材料及工艺研究所，北京 100076）

摘 要： 炭纤维增强树脂基复合材料（CFRP）的轴向压缩强度显著低于其拉伸强度，这阻碍了其更广泛的应用。CFRP 的轴向压缩破坏机理复杂，而目前针对 CFRP 轴向压缩破坏的研究却较为有限。为了对 CFRP 轴向压缩破坏机制有更加深入且直观的理解，本文构建了一个二维的微观有限元模型。该模型能够完整揭示 CFRP 轴向压缩破坏过程，并预测纤维和基体各项性能对 CFRP 抗压强度的影响规律。结果证明，由纤维初始制造缺陷引起的剪切应力集中使得基体开始发生塑性屈服，并最终形成扭折带，材料结构失效。剪切应力在整个失效过程中扮演着重要角色。此外，本文系统研究了纤维和基体各项性能对 CFRP 的抗压强度的影响，这些性能包括纤维轴向弹性模量 E_{f1}、纤维径向弹性模量 E_{f2}、纤维剪切模量 G_{f12}、基体弹性模量 E_m、基体比例极限 σ_p、基体屈服强度 σ_s 和纤维初始制造缺陷程度。研究发现，性能的变化直接影响着缺陷区域剪切应力的集中状态，从而影响 CFRP 的抗压强度。研究结果显示，当 E_{f1}、E_{f2}、G_{f12}、E_m、σ_p、σ_s 提升 10%，纤维初始缺陷程度降低 10% 时，CFRP 的抗压强度分别提升了 2.33%、0、0.39%、3.38%、1.17%、2.30%、2.52% 左右。研究了 CFRP 抗压强度对各参数的敏感性，结果发现，E_m 对 CFRP 的抗压强度影响最大，纤维的初始制造缺陷程度和基体的塑性性能也是不可忽略的因素。

关键词： 炭纤维增强树脂基复合材料（CFRP）；抗压强度；参数灵敏度；有限元模拟；扭折带

中图分类号： TB332 **文献标识码：** A

基金项目：国家自然科学基金（21676163）；航空科学基金（2017ZFS6001）；先进功能复合材料技术重点实验室基金（614290601011811）.

通讯作者：张方舟，博士，讲师. E-mail：zhangfzh@shu.edu.cn

作者简介：李爱军，教授. E-mail：aijun.li@shu.edu.cn

Effects of fiber and matrix properties on the compressive strength of carbon fiber reinforced polymer composites

LI Ai-jun[1,2], ZHANG Jun-jun[1], ZHANG Fang-zhou[2], LI Long[3], ZHU Shi-peng[3], YANG Yun-hua[3]

（1. *School of Materials Science and Engineering, Shanghai University, Shanghai* 200444, *China*;
2. *Institute of Materials, Shanghai University, Shanghai* 200072, *China*;
3. *Institute of Space Materials and Technology, Beijing* 100076, *China*）

Abstract: The axial compressive strength of carbon fiber reinforced polymer composites (CFRP) is significantly lower than the tensile strength, which hinders its wide applications. The failure mechanism of CFRP under unidirectional compression parallel to the fiber alignment direction is complex, but research on this issue is limited. In order to understand this mechanism more deeply and intuitively, a two-dimensional microscopic numerical model is proposed. The influences of various properties of the fiber and matrix on the compressive strength of CFRP are investigated, including the axial elastic modulus of the fiber (E_{f1}), the transverse elastic modulus of the fiber(E_{f2}), the shear modulus of the fiber (G_{f12}), the elastic modulus of the matrix (E_m), the proportional strength limit of the matrix (σ_p), the yield strength of the matrix (σ_s) and the degree of initial fiber misalignment. Results show that the model is capable of explaining the failure mechanism of CFRP under a unidirectional compressive load. Shear stress plays an important role in the compressive failure process. The localization of shear stress caused by initial fiber misalignment leads to plastic yield of the matrix and finally a kink band. Changes in these properties directly affect the concentration of shear stress in the defect areas, thereby affecting the compressive strength of the CFRP. When the values of E_{f1}, E_{f2}, G_{f12}, E_m, σ_p, σ_s are separately increased by 10% or the degree of initial fiber misalignment is decreased by 10%, the compressive strength of CFRP is increased by 2.33%, 0, 0.39%, 3.38%, 1.17%, 2.30% and 2.52% respectively. E_m has the greatest influence on the compressive strength of CFRP, followed by the initial fiber misalignment. The effects of the plastic properties of the matrix on the compressive strength of CFRP are obvious.

Key words: Carbon fiber reinforced polymer composites (CFRP); Compressive strength; Finite element simulation; Kink-band; Parameter sensitivity

Received date: 2019-10-12; *Revised date*: 2020-03-02
Foundation items: National Natural Science Foundation (21676163); Aviation Science Foundation (2017ZFS6001); Science and Technology on Advanced Functional Composites Laboratory Funding (614290601011811).
Corresponding author: ZHANG Fang-zhou, Ph. D, Lecturer. E-mail: zhangfzh@shu.edu.cn
Author introduction: LI Ai-jun, Professor. E-mail: aijun.li@shu.edu.cn

1 Introduction

Carbon fiber reinforced polymer (CFRP) composites are important materials in many fields such as aerospace, medical equipment, and automobile manufacturing owing to their excellent specific strength and modulus. However, research shows that the axial compressive strength of unidirectional CFRP is much lower than the tensile strength[1,2], which limits the wide applications of CFRP. Experimental studies on the axial compression failure of CFRP illustrate that fiber kinking is the most common failure mode[3-5]. It has been showed that fiber kinking is closely related to the initial fiber misalignment[1]. Vogler and Kyriakides[6] applied compressive and shear load on the unidirectional specimen and observed the quasi-static growth of kink bands across composite plates, indicating the important role of shear stress in fiber kinking. Moran et al[7] also observed almost stable in-plane extensions of kink-band by compressing CFRP specimens with single notched edges. A typical micrograph of kink-band is shown in Fig. 1.[8]

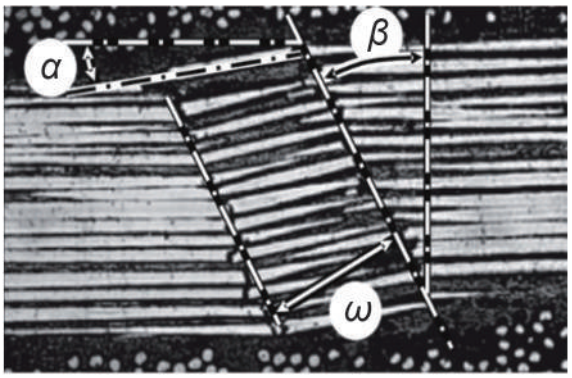

Fig. 1 Typical kink-band micrograph from experiments: rotation angle of fiber α, angle of kink band β, width of kink band ω[8].

Rosen[9] first proposed an analytical theoretical method to predict the compressive strength of fiber reinforced composites. However, he assumed an elastic buckling theory of aligned fibers without considering the fiber initial misalignment. As a result, the predicted results of the model are always higher than experimental ones. Argon[10] and Budiansky et al[11] improved the Rosen's theory by introducing the initial fiber misalignment into their analytical model, which brought their results closer to the experimental values. They believed that the shear stress caused by the initial fiber misalignment leads to slide and rotation of the fiber, which is the main cause of the formation of kink-band. Their research was later recognized by many researchers.

In recent years, finite element (FE) models have been developed in order to further understand the compression failure mechanism of CFRP. Basu et al[12] idealized CFRP as a two-dimensional plane formed by alternating fiber layers and matrix layers, and captured the formation of kink-band through a finite element method. Pimenta et al[3] and Bishara et al[13,14] considered the fiber fracture and matrix plasticity in their model, and simulated the formation and expansion of the kink-band. Their results indicated that the plastic yield of the matrix plays a key role in the formation of the kink-band and the failure of the fibers first occurs at the edge of the kink-band. In the work of Vogler et al[15] and Bishara et al[13], models with local and global fiber initial imperfections were used to study the initiation and growth of the kink-band, respectively by a numerical simulation method. Their research showed that both local and global imperfections can induce kink-band, but local imperfections are more likely to produce kink-band with obvious characteristics. The study also suggests that the final angle of the kink-band is dominated by the tensile strength of the fiber. Yerramalli and Waas[16] presented a three-dimensional model to study the effect of the fiber diameter on the compressive strength of CFRP. The results demonstrate that the compressive strength increases with the increase of the fiber diameter, which has been verified by their experiments. More importantly, they also found that there is no obvious difference between the predicted compressive strength based on 2D and 3D models. Zhou et al[17] proposed a 2D model in which global imperfection was introduced and the plastic yield of the matrix was considered. In addition to compressive failure mechanism, the effects of the fiber volume fraction, the initial fiber misalignment, the initial fiber-matrix interface sti ness, the interface strength and the fracture energies on compressive strength were studied.

Researchers have been committed to obtain models that can be generally accepted using whether analytical methods or numerical simulation methods. Despite of the above understanding, it remains some unclear topics on the compressive failure of CFRP. What remains unclear is the extent to which the changes in mechanical properties of fibers and matrix affect the compressive strength of CFRP. To answer the question and expound the compression failure mechanism of CFRP, we presented our numerical investigations on the axial compressive failure of unidirectional CFRP. A 2D microscale FE model with local initial fiber misalignment was developed. The sensitivity of the compressive strength to various mechanical properties was studied in order to understand the influence of each mechanical property on the compressive strength. The property of carbon fibers is heterogeneous. Although some researchers have taken this into account, no detailed studies have been done in this regard. In the paper, the influence of anisotropic stiffness of fibers in different directions was also discussed. Therefore, the parameters related to the mechanical properties of the fiber include the axial elastic modulus of fiber (E_{f1}), the transverse elastic modulus of fiber (E_{f2}), and the shear modulus of fiber (G_{f12}). The mechanical parameters related to the matrix include the elastic modulus of matrix (E_m), the proportional limit of matrix (σ_p) and the yield strength of matrix (σ_s). In addition, the effect of the initial fiber misalignment on the compressive strength was also studied.

2 Modelling

2.1 Geometric model

The model idealizes CFRP as a two-dimensional plane with two independent components of alternating fiber layers and matrix layers, as shown in Fig. 2. The width of the fiber layer (d_f) is assumed to be 5.1 μm. According to the fiber volume fraction which is 60%, the width d_m of matrix layer can be deduced to be equal to 3.4 μm. After studying the rationality of the model, according to the previous study, the number of fibers was assumed to be 22 in order to capture the kink-band. The local fiber imperfections were introduced as a half sinusoidal waviness, making the transition from the defect zone to the defect-free zone smoother. As shown in Fig. 3, the length of the imperfection zone (L) is 25 μm, far less than the length of the entire structure (x), 1 025 μm, and λ represents the amplitude. λ/L is assumed to be 0.012 5, indicating the degree of imperfection.

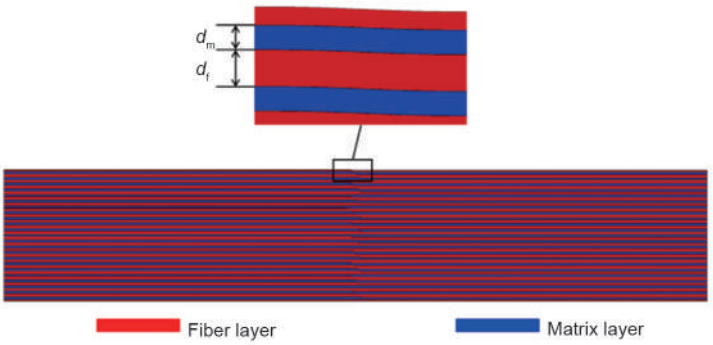

Fig. 2 Geometric model.

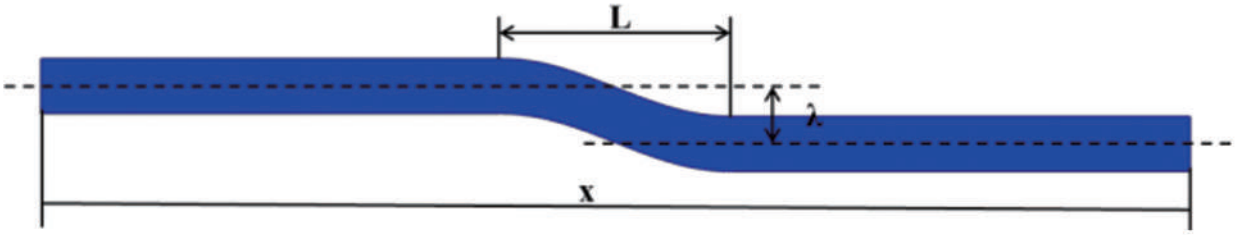

Fig. 3 Schematic diagram of local imperfection.

2.2 Material model

The carbon fiber in the model was assumed to be an orthotropic and elastic material. The properties of fiber are given in Table 1. The axial modulus of the fiber is the data of Toray T800 carbon fiber obtained in the experiment[18]. Other properties were referenced from the transverse and shear modulus of T300 carbon fiber measured by Hiroaki Miyagawa et

al[19,20], because the data on the shear modulus and transverse modulus of T800 carbon fiber is still not available. Unlike the axial modulus of the fiber, the characterization of the transverse and shear modulus of the fiber has always been a challenging problem, and there is currently no generally accepted standard test method. The matrix in the model was considered to be an elastoplastic material. The elasticity and the plasticity of the matrix were characterized from the axial compressive behavior of a 603 epoxy polymer, as shown in Fig. 4. The Young's modulus of the matrix was identified as 4 710 MPa and the plasticity of the matrix were derived from the plastic section of the curve.

Table 1　Mechanical properties of fibers.

E_{f1}/MPa	E_{f2}/MPa	ν_{12}	ν_{23}	G_{f12}/MPa	G_{f23}/MPa
290000	8000	0.256	0.3	27300	3080

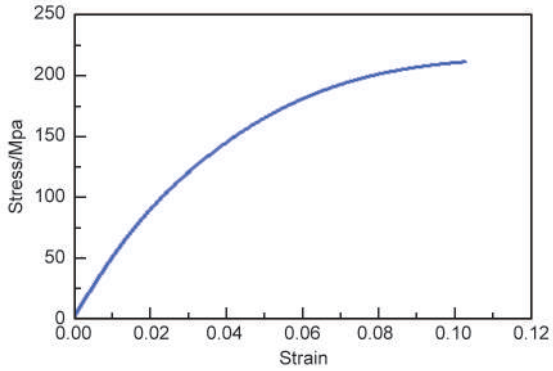

Fig. 4　Stress-strain curve of matrix.

2.3　Finite element model

The commercial finite element software ABAQUS is used to simulate the compression process of CFRP. The finite element model is shown in Fig. 5. The fibers and the matrix in the model were meshed with linear plane strain continuum elements CPE4. Three elements were laid along the width of each fiber or matrix layer. Considering the severity of deformation in the defective area, in order to increase the reliability of simulation, from both sides to the inside, the mesh size gradually decreases from 25 to 0.5 μm. The left end of the model has a boundary condition of zero displacement in the fiber direction, the upper left end is fully constrained, and the right end is given a compression displacement. Due to the convergence difficulty generated by fiber kinking, the compression process was simulated using the explicit module of ABAQUS.

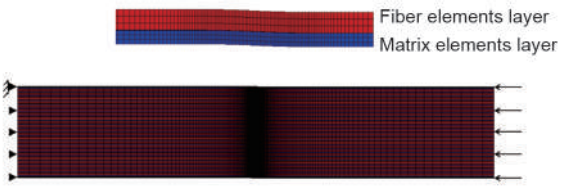

Fig. 5　Finite element model.

2.4　Computational scheme

Based on the above-mentioned parameters, a baseline model was established to explain the axial compression failure mechanism of CFRP. Furthermore, the simulation results of the baseline model were compared with the experimental ones to validate the model. The effects of the mechanical properties of the fiber and the matrix on the compressive strength of CFRP were then investigated. The performance parameters include the axial elastic modulus of the fiber (E_{f1}), the radial elastic modulus of the fiber (E_{f2}), the shear modulus of the fiber (G_{f12}), the elastic modulus of the matrix (E_m), the proportional limit of the matrix (σ_p), the yield strength of matrix (σ_s) and the degree of initial fiber misalignment. The variations of the above parameters take the changes of −10%, −5%, +5%, +10% relative to the benchmark model. The sensitivity of the compressive strength to various parameters is studied.

3　Results and discussion

3.1　Compression failure mechanism of CFRP

The compressive strength predicted by this baseline model is 1 669.7 MPa while the experimental result is 1 680 MPa[18]. The slight difference between the experimental and simulated values indicates that the model can predict the compressive strength of CFRP. The experimental specimens were prepared from Toray T800 carbon fiber and 603 epoxy resin. The size of the sample is made according to the compression test standard ASTM D3410-03[21], which is $150 \times 10 \times 3$ mm^3. The total length of the sample includes a gage length of 20 mm and tab length of 65 mm at both ends. The fiber volume fraction of the specimen is 60%, which is consistent with the model. The porosity of the sample is less than 3%.

The stress-strain curve obtained from the baseline model is illustrated in Fig. 6. The stress-strain response is linear until a critical stress, after which the stress drops suddenly and the material structure fails instantaneously. Due to the adoption of the ABAQUS/Explicit dynamics module, a small oscillation phe-

nomenon occurs at the end of the curve. Fig. 7 shows the distributions of shear stress S_{12} at different stages of compression corresponding to points 1-4 on the curve in Fig. 6. Due to the existence of the initial fiber misalignment, shear stress concentration occurs in the defect zone. The shear stress concentration area continuously expands with increasing load, and eventually passes through the entire model in the width direction, which causes the final formation of kink-band and the failure of the material structure. Therefore, shear stress plays an important role in the whole failure process. In addition, on both sides of the kink-band, the fibers are significantly bent, as shown in Fig. 8. Although the material as a whole is in compression, the fibers on both sides are subject to tensile stress, which can be verified from the experiments of Pimenta et al[3]. Open cracks in the fibers on both sides of the kink band can be observed in Fig. 9. Their research also proves, at the outer edges, that the fibers reach the tensile strength first at both sides of the kink band.

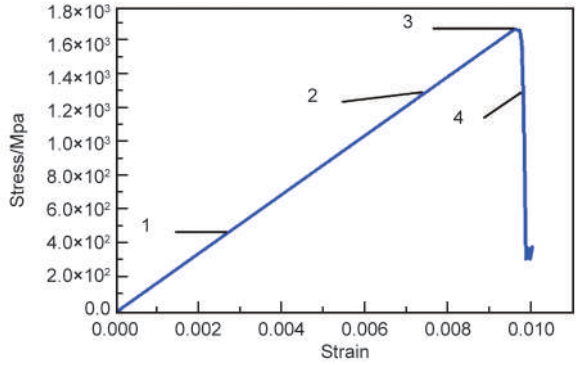

Fig. 6 Stress-strain curves obtained from CFRP unidirectional compression simulation.

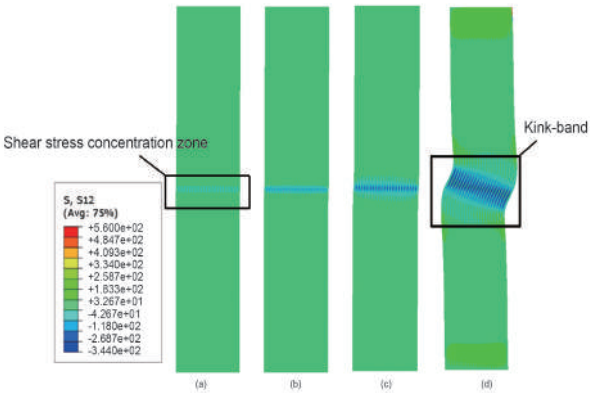

Fig. 7 (a) Shear stress begins to appear (point 1), (b) Extension of shear stress (point 2), (c) Shear stress state at peak point (point 3) and (d) Shear stress state of kink-band (point 4).

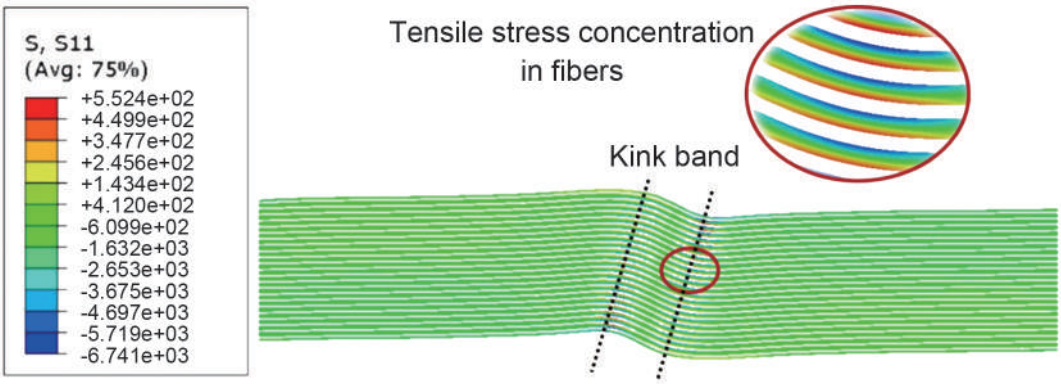

Fig. 8 Stress distribution map of fibers in fiber direction.

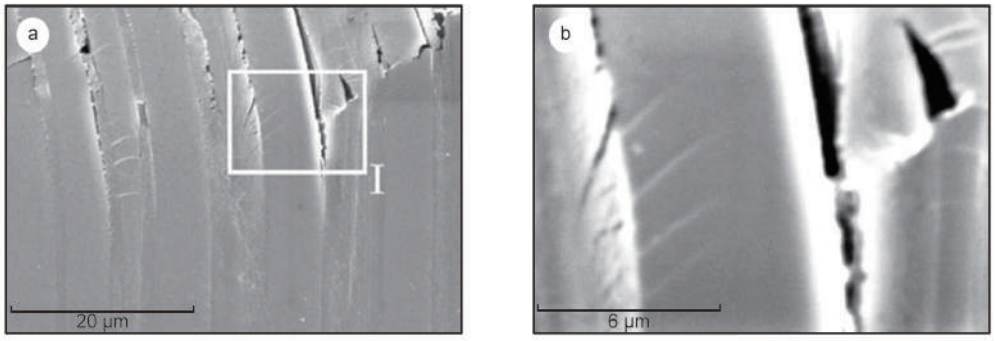

Fig. 9 Edge of kink-band and fracture of fibers[3]: (a) Edge of kink-band and (b) An enlarged view of region I.

The plastic properties of the matrix are introduced into the model, and the concentration of shear stress causes the matrix to yield plastically. Before the formation of the kink-band, the onset and growth of the plastic yield of the matrix can be clearly observed (Fig. 10). Similarly, Fig. 10 (a), Fig. 10 (b), Fig. 10 (c), and Fig. 10 (d) correspond to points 1-4 in Fig. 6, respectively. The plastic yield of matrix starts at the initial fiber imperfection zone and expands continuously under compressive load. When the yield continues to occur, the fiber gradually loses the support from the matrix, and the kinking behavior occurs. When the yield band passes through the entire width, a kink-band is formed. The morphology of the kink-band obtained by simulation is very similar to that observed by previous experiments[3-5]. During the kinking process, the phenomenon that the fibers are locally subjected to concentrated tensile stress appears after the formation of kink-band, which indicates that the primary cause of the material structure failure is not the failure of fibers, but the plastic yield behavior of the matrix.

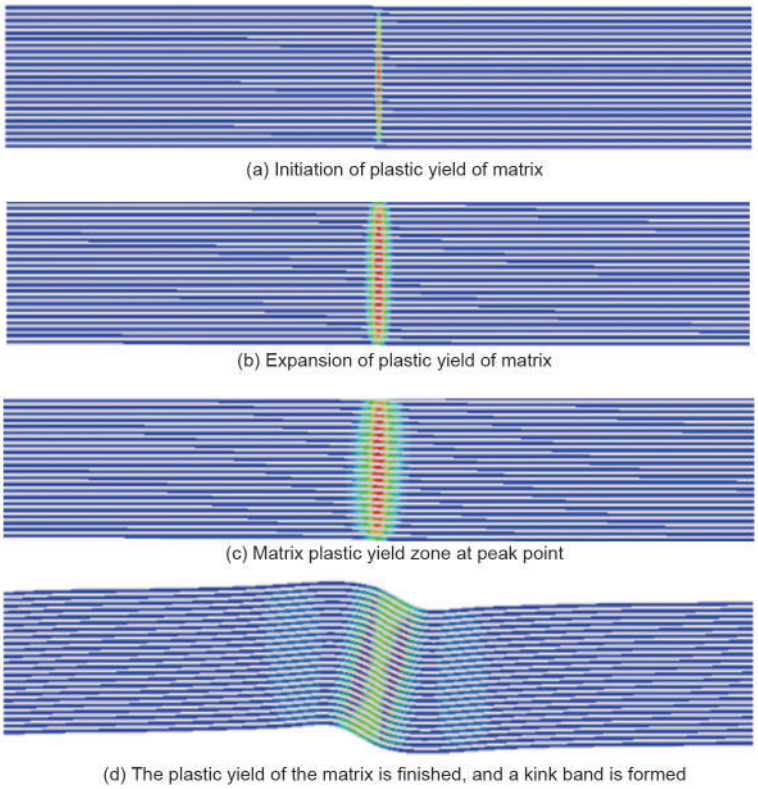

Fig. 10　Initiation, expansion and end of plastic yield of matrix.

3.2　Results of parametric studies

3.2.1　Influence of the elastic modulus of the matrix

Fig. 11 shows the variation of the compressive strength versus E_m. The compressive strength increases linearly with the increase of E_m. It indicated that a lower E_m can cause earlier material structural failure and smaller failure strain. In the model, the matrix is assumed to be isotropic and elastic material. Therefore, the shear modulus G_{m12} of matrix is also improved while E_m is increased, which makes the matrix more resistant to deformation and increases the compressive strength of CFRP accordingly. It is further proved that the concentrated shear stress is the reason for the plastic yield of the matrix.

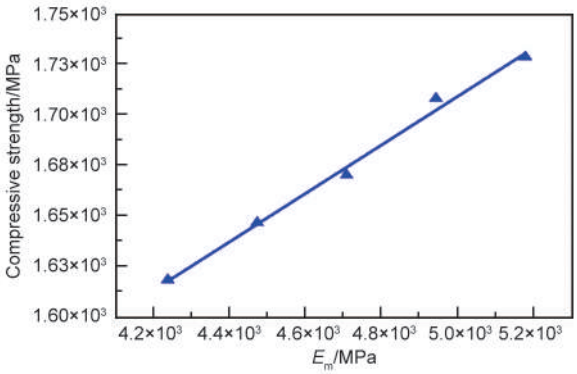

Fig. 11　Influence of E_m on the compressive strength.

3.2.2　Influence of the yield strength of the matrix

According to the axial compression stress-strain curve of 603 epoxy resin (Fig. 4), the proportional limit of the matrix (σ_p) was kept consistent with the baseline model, which is 50 MPa, and the yield

strength of the matrix was varied within a range of ±10%. The plastic stage of the stress-strain curve of the matrix with different yield strengths is drawn in Fig. 12. The predicted compressive strength versus the yield strength of the matrix is plotted in Fig. 13. The result shows that the compressive strength of CFRP increases almost linearly with the increase of σ_s. The increase of σ_s causes the plastic yield zone of the matrix to propagate more slowly, which results in the improvement of the compressive strength of CFRP.

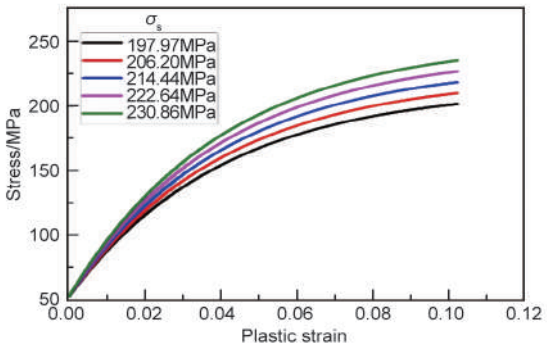

Fig. 12 Plastic section curve of matrix with different yield strengths.

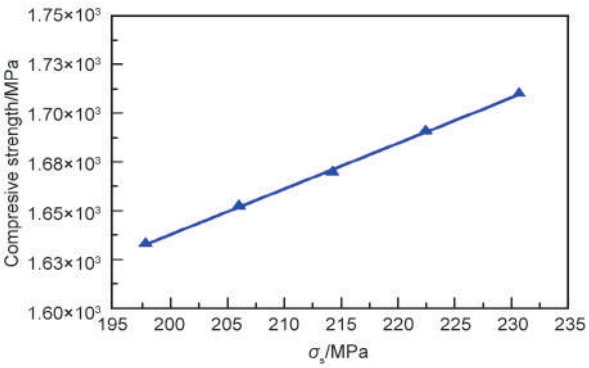

Fig. 13 Effect of σ_s on the compressive strength.

3.2.3 Influence of the proportional limit of the matrix

In the same way, according to the axial compression stress-strain curve of 603 epoxy resin (Fig. 4), in order to explain the influence of σ_p on the compressive strength, σ_p is changed within a range of ±10%, while the yield strength of matrix (σ_s) remains unchanged. The plastic stage of the stress-strain curve of the matrix with different proportional limits is drawn in Fig. 14. As shown in Fig. 15, the compressive strength of CFRP increases with the increase of σ_p, because the increase of σ_p enhances the yield resistance of the matrix.

3.2.4 Influence of the axial elastic modulus of the fiber

Fig. 16 illustrates the influence of the axial elastic

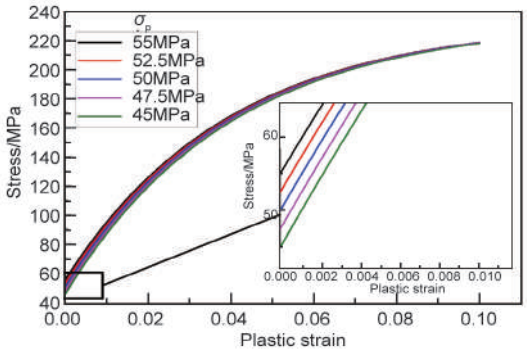

Fig. 14 Matrix plastic section curves with different proportional limits.

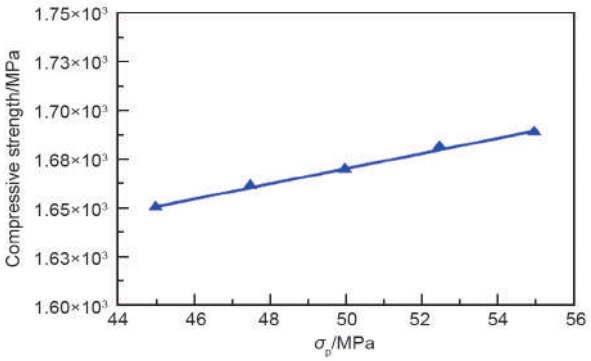

Fig. 15 Influence of σ_p on the compressive strength.

modulus of the fiber (E_{f1}) on the compressive strength. It is observed that E_{f1} has a positive influence on the compressive strength. Fig. 17 exhibits the compressive response of CFRP with different axial elastic modulus E_{f1} of the fiber. In Fig. 17, the stiffness of the whole material is improved due to the increase of E_{f1}, which is the main reason why the compressive strength of CFRP increases with the increase of E_{f1}. In addition, while the compressive strength of CFRP is improved, the failure strain is reduced and the material failure is advanced. This phenomenon can be explained by variation of the shear stress. Table 2 shows the shear stress value of the same element under the same global strain when E_{f1} changes. The increase of E_{f1} enhances the shear stress in the stress concentration area, which causes the compression response curve to reach the peak point faster.

3.2.5 Influence of the transverse elastic modulus of the fiber

Fig. 18 illustrates the fact that the transverse elastic modulus of the fiber has no effect on the compressive strength of CFRP.

3.2.6 Influence of the shear modulus of the fiber

The predicted compressive strength versus the shear modulus of the fiber (G_{f12}) is plotted in Fig. 19. The result of fitting the data to the curve indicates that G_{f12} is almost proportional to the

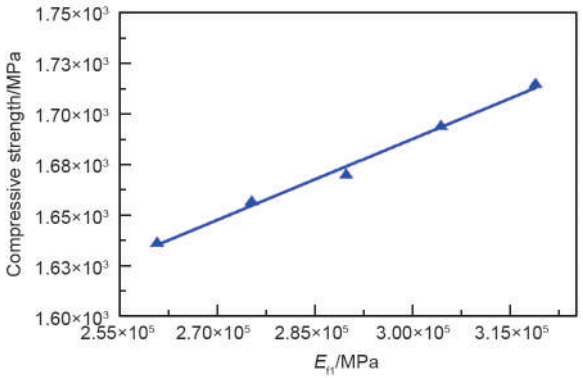

Fig. 16　Influence of E_{f1} on the compressive strength of CFRP.

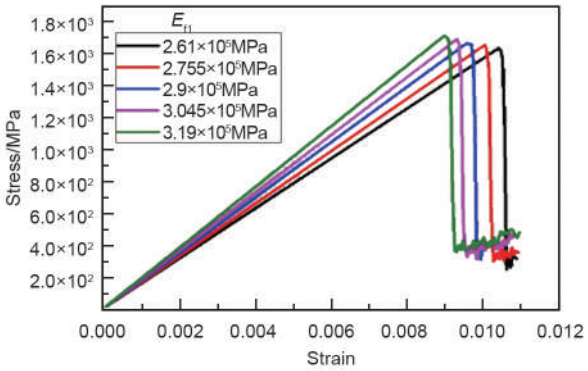

Fig. 17　Compressive stress-strain curves of CFRP with different E_{f1}.

Table 2　Shear stress of the same element under the same strain.

Changes in E_{f1}	−10%	−5%	0	5%	10%
Shear stress/MPa	91.280	99.214	108.754	115.538	124.451

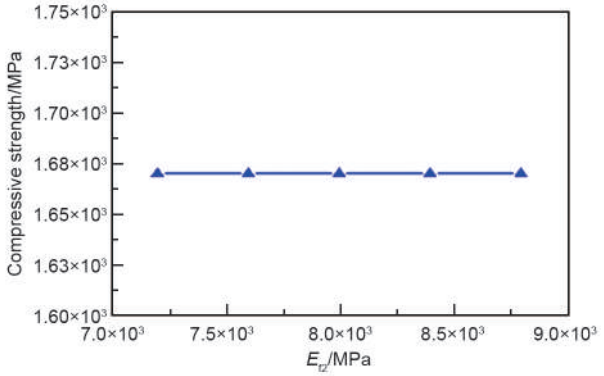

Fig. 18　Influence of E_{f2} on the compressive strength of CFRP.

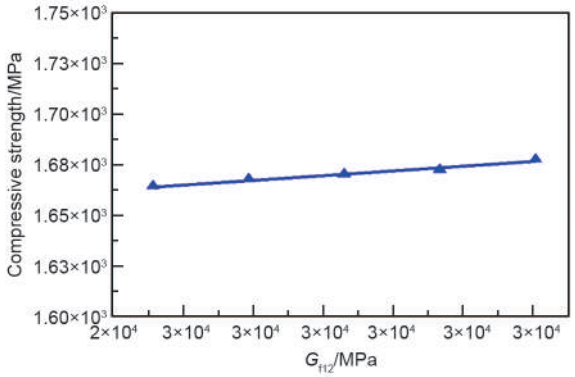

Fig. 19　Influence of G_{f12} on the compressive strength of CFRP.

compressive strength of CFRP. In terms of this parameter, the shear modulus of the whole material structure is increased due to the fact that the increase of G_{f12} is the reason why the compressive strength of CFRP is improved. Also, the improvement of shear properties of the whole material structure makes the yield of the defective area more difficult.

3.2.7　Influence of the initial fiber misalignment

The model use λ/L to represent the level of initial fiber misalignment. The predicted compressive strength versus the degree of initial fiber misalignment is shown in Fig. 20. The compressive strength of CFRP reduces sharply with the increase of λ/L. The existence of the initial fiber misalignment facilitates the concentration of the shear stress in matrix, resulting in the plastic yield of the matrix easily. In addition, a high degree of initial fiber misalignment will enhance the concentration of shear stress, leading to an earlier reaching of the failure strain in the pressurized material and a lower compressive strength value.

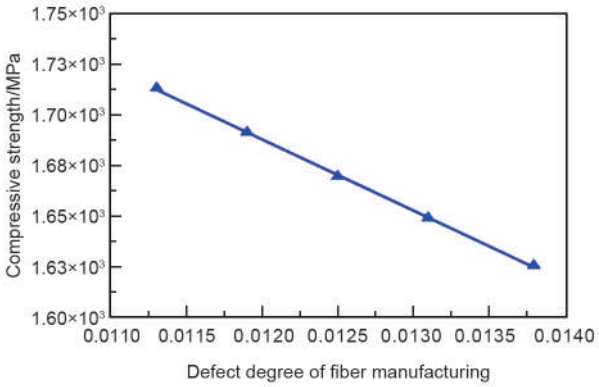

Fig. 20　Influence of λ/L on the compressive strength of CFRP.

3.3　Sensitivity analysis of the compressive strength of CFRP to various parameters

The compressive strength of CFRP is taken as the function of the variation range of the parameter. The fitting curve is shown in Fig. 21 to illustrate the relationship between the parameter variation and the compressive strength. When the parameter changes by 10%, the change of compressive strength is defined as the sensitivity value of the compressive strength to the parameter. The sensitivity value K is expressed as

$$K = \frac{\Delta\sigma_i}{\sigma_0} \quad (1)$$

where i represents a studied parameter, $\Delta\sigma_i$ is the variation of the compressive strength when the parameter changes by 10%, and σ_0 is the predicted compressive strength value of the baseline model.

The K sensitivities corresponding to the parameters E_{f1}, E_{f2}, G_{f12}, E_m, σ_p, σ_s and the initial fiber misalignment are 2.33%, 0%, 0.39%, 3.38%, 1.17%, 2.30% and 2.52%, respectively, as shown in Fig. 22. It can be seen that E_m has the greatest influence on the compressive strength of CFRP, followed by the initial fiber misalignment. Besides, E_{f2} has no effect on the compressive strength of CFRP and the influence of plastic properties of matrix cannot be ignored.

Here, the weak influence of G_{f12} on the compressive strength of CFRP is explained by the effect of G_{f12} on the shear modulus of composite material, which can be estimated by the following equation (2).

$$\frac{1}{G_{c12}} = \frac{1}{G_{f12}} + \frac{1}{G_{m12}} \quad (2)$$

where G_{m12} is the shear modulus of matrix. In Eq. (2), compared with $1/G_{f12}$, $1/G_{m12}$ has a more significant influence because G_{m12} is much smaller than G_{f12}. The improvement of G_{c12} will enhance the yield resistance of the material, which will improve the compressive properties of the material. Therefore, G_{m12} has a more significant effect on the compressive strength of CFRP than G_{f12}.

The discussion in this section shows that improving the elastic and plastic properties of the matrix is of great significance to improve the compressive strength of CFRP. In addition, reducing the degree of initial fiber misalignment in the production process can also effectively improve the axial compression performance of CFRP.

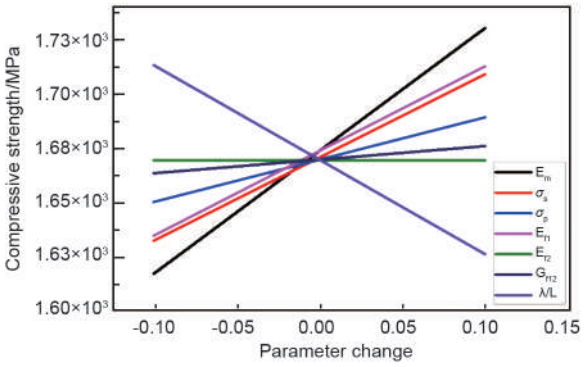

Fig. 21 Influence of parameter changes on the compressive strength.

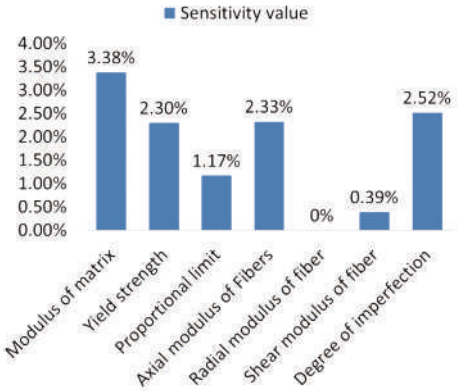

Fig. 22 Sensitivity of parameters.

4 Conclusion and prospect

This work proposed a 2D micromechanical model to investigate the axial compressive failure mechanisms of carbon fiber reinforced polymer (CFRP) composites. The developed model performs well on predicting the compressive strength of CFRP and capturing initial and growth of the kink-band. A few conclusions are as follows.

(1) Compression failure mechanism of CFRP: Under the effect of an axial compressive load, the existence of initial fiber misalignment leads to a significant shear stress concentration, which will cause the plastic yield of the matrix. With the continuous yielding of the matrix, the matrix gradually loses its ability to support the fibers, causing the fibers to kink. Eventually, a kink-band is formed at the imperfection and structural failure of materials occurs. The primary cause of CFRP axial compression failure is the plastic yield behavior of matrix caused by a shear stress concentration rather than the fiber fracture.

(2) The influence of various parameters on the compressive strength of CFRP is summarized as follows: The influences of E_m, σ_p, σ_s, E_{f1}, G_{f12} and on the compressive strength of CFRP are positive, while the influence of initial fiber misalignment on the compressive strength of CFRP is negative. And the transverse elastic modulus E_{f2} of the fiber has no effect on the compressive strength of CFRP. When E_{f1}, E_{f2}, G_{f12}, E_m, σ_p, σ_s are increased by 10% and the initial fiber misalignment is reduced by 10%, the compressive strength of CFRP is increased by 2.33%, 0%, 0.39%, 3.38%, 1.17%, 2.30% and 2.52%, respectively.

(3) According to the discussion in section 3.3, the elastic modulus of the matrix (E_m) has the greatest influence on the compressive strength of CFRP, followed by the initial fiber misalignment. The effects of the plastic properties of matrix cannot be ignored either. Therefore, in practical production, it is reasonable to improve the axial compressive performance

of CFRP by minimizing the initial fiber misalignment and enhancing the mechanical properties of the resin.

Compared with the tensile properties of CFRP, the understanding of the compression properties and compression failure mechanism of CFRP still needs to be improved. This study focuses on the influence of the mechanical properties of fibers and matrix on the compressive strength of CFRP. In the following, we will further discuss the influence mechanism of interface performance, damp – heat aging and other factors on the compression performance of CFRP based on the presented model. In addition, experiments will be carried out to validate the prediction accuracy of the model.

References

[1] Budiansky B, Fleck N A. Compressive failure of fibre composites [J]. Journal of the Mechanics and Physics of Solids, 1993, 41(1): 183-211.

[2] SHI Pei-luo, WANG Yue-you, GUO Hong-jun, et al. The thermal and mechanical properties of carbon fiber/flake graphite/cyanate ester composites [J]. New Carbon Materials, 2019, 34(1): 110-114.

[3] Pimenta S, Gutkin R, Pinho S, et al. A micromechanical model for kink-band formation: Part I-Experimental study and numerical modelling [J]. Composites Science and Technology, 2009, 69(7-8): 948-955.

[4] Gutkin R, Pinho S T, Robinson P, et al. Physical mechanisms associated with initiation and propagation of kink-bands: proceedings of the Proceedings of the 13th European conference on composite materials (ECCM13) [C], F, 2008.

[5] Vogler T, Kyriakides S. On the axial propagation of kink bands in fiber composites: Part I experiments [J]. International journal of solids and structures, 1999, 36(4): 557-574.

[6] Vogler T, Kyriakides S. On the initiation and growth of kink bands in fiber composites: Part I. experiments [J]. International journal of solids and structures, 2001, 38(15): 2639-2651.

[7] Moran P, Liu X, Shin C. Kink band formation and band broadening in fiber composites under compressive loading [J]. Acta Metallurgica et Materialia, 1995, 43(8): 2943-2958.

[8] Pimenta S, Gutkin R, Pinho S T, et al. A micromechanical model for kink-band formation: Part II-Analytical modelling [J]. Composites Science and Technology, 2009, 69(7-8): 956-964.

[9] Rosen W. Mechanics of Composite Strengthening [J]. Fiber Comopsite Materials, 1964, 72.

[10] Argon A S. Fracture of composites[J]. Treatise on materials science and technology, 2013, 1: 79-114.

[11] Budiansky B, Fleck A. Compressive kinking of fiber composites: a topical review [J]. Appl Mech Rev, 1994, 47(6): S246-S270.

[12] Basu S, Waas A, Ambur D. A macroscopic model for kink banding instabilities in fiber composites [J]. Journal of Mechanics of Materials and Structures, 2006, 1(6): 979-1000.

[13] Bishare M, Rolfes R, Allix O. Revealing complex aspects of compressive failure of polymer composites-Part I: Fiber kinking at microscale [J]. Composite Structures, 2017, 169: 105-115.

[14] Bishara M, Vogler M, Rplfes R. Revealing complex aspects of compressive failure of polymer composites-Part II: Failure interactions in multidirectional laminates and validation [J]. Composite Structures, 2017, 169: 116-128.

[15] Vogler T, Hsu S Y, Kyriakides S. On the initiation and growth of kink bands in fiber composites. Part II: Analysis [J]. International Journal of Solids and Structures, 2001, 38(15): 2653-2682.

[16] Yerramalli C S, Waas A M. The effect of fiber diameter on the compressive strength of composites-A 3D finite element-based study [J]. Computer Modeling in Engineering and Sciences, 2004, 6: 1-16.

[17] Zhou L, Zhao L, Liu F, et al. A micromechanical model for axial compressive failure in unidirectional fiber reinforced composite [J]. Results in Physics, 2018, 10: 841-848.

[18] LI Y Y, Zhang F, Zhu S, et al. Investigation on improving the Compressive Strength of the Unidirectional Carbon Fiber Reinforced Polymer Composite: Twenty-second international conference on composite material (ICCM22), 2019 [C].

[19] Miyagawa H, Sato C, Mase T, et al. Transverse elastic modulus of carbon fibers measured by Raman spectroscopy [J]. Materials Science and Engineering: A, 2005, 412(1-2): 88-92.

[20] Miyagawa H, Mask T, Sato C, et al. Comparison of experimental and theoretical transverse elastic modulus of carbon fibers [J]. Carbon, 2006, 44(10): 2002-2008.

[21] Standard A. D3410-03 (2008). Compressive Properties of polymer matrix composite materials with unsupported gage section by shear loading," [S]. ASTM International (W Conshohocken, Pa), 2008.